Observing cross-channel NLI generation in disaggregated optical line systems

Observing cross-channel NLI generation in disaggregated optical line systems

Elliot London[1*], Emanuele Virgillito[1], Andrea D'Amico[1], Antonio Napoli[2] and Vittorio Curri[1]

[1]*DET, Politecnico di Torino, Corso Duca degli Abruzzi 24, 10129 Torino, Italy;* [2]*Infinera Ltd, London, UK*

[*]*elliot.london@polito.it*

Abstract: We investigate spatially separated XPM generation in a wide variety of 400G-ZR+ 64GBd pump-and-probe simulations, demonstrating the existence of a per-span upper bound that depends solely upon accumulated dispersion.

1. Introduction

Rapidly increasing internet traffic demands [1] must be addressed by maximizing optical network capacities and throughputs, first by ensuring that existing network infrastructures are maximally exploited. Networks are hence undergoing progressive hardware upgrades, in particular to devices that are able to transmit data according to 400G-ZR+, permitting use of a 4.8 THz bandwidth with channels transmitting 64 GBd signals within a 75 GHz, wavelength division multiplexing (WDM) grid. In tandem with these upgrades, networks are shifting towards open and disaggregated architectures, where signals are transmitted through optical line systems (OLS)s over independent lightpaths (LP)s by multiple vendors using disaggregated, re-configurable optical add-drop multiplexers (ROADM)s. Estimating quality of transmission (QoT) of each transparent lightpath is essential in assessing network performance and is a quantity which is well approximated by the generalized signal-to-noise ratio [2]:

$$\mathrm{GSNR}^{-1} = \mathrm{OSNR}^{-1} + \mathrm{SNR}_{\mathrm{NL}}^{-1}, \tag{1}$$

where OSNR quantifies the amplified spontaneous emission (ASE) noise arising from the amplifiers, and $\mathrm{SNR}_{\mathrm{NL}}$ quantifies the accumulated nonlinear crosstalk during propagation through the fiber spans, namely the nonlinear interference (NLI). The NLI can be separated into its constituent terms [3]: self-phase modulation (SPM), cross-phase modulation (XPM) and other four wave mixing (FWM) contributions, with the latter being negligible for most realistic transmission scenarios [4].

Aggregated NLI models, such as the enhanced Gaussian noise model (EGN) [5], approach point-to-point transmission assuming full knowledge of the system under investigation, providing excellent accuracy over a wide range of network configurations, however NLI modelling in a disaggregated network scenario requires an equally disaggregated approach for multiple reasons. Firstly, vendors may not be willing to disclose essential spectral or device information due to privacy reasons, significantly inhibiting the model accuracy. Furthermore, shared network infrastructures enable the potential for alien wavelengths – channels operated by a third-party vendor that may have unknown source and/or destination nodes within the network [6]. These alien wavelengths present a fundamental issue for NLI quantification, as this is a non-local quantity that depends upon the LP history. These issues are lessened when NLI modelling is approached from a disaggregated standpoint, where channels are fundamentally treated separately; the XPM of each pump may be superimposed, along with the SPM by considering its coherency [7], accurately accounting for full-spectrum effects in a spectrally and spatially separated manner [8], as required by channels with unknown parameters and history.

Within this paper we investigate the generation of XPM in multiple simulated pump-and-probe scenarios in the presence of varying amounts of accumulated dispersion. We evaluate the amount of NLI that is generated by wavelengths originating from sources of varying distance away from the OLS under investigation, in order to maximally quantify the NLI generated for a given span. These simulations are performed using an internal simulation framework that solves the dual polarization Manakov equation [9]. Furthermore, we extend the investigation performed in [8] to mixed-fiber scenarios, where the chromatic dispersion of fiber spans within the OLS differs, in order to consider XPM generation in non-uniform OLS configurations, such as what may be expected within realistic terrestrial network scenarios.

2. Split-Step Fourier Method (SSFM) Simulation Campaign

To evaluate the XPM generated in various pump-and-probe configurations we set up a common SSFM framework that was used for all configurations within this article. We considered a single interfering channel 150 GHz distant

from a single channel under test (CUT), located at 194.05 THz and 193.9 THz, respectively, each with channel bandwidths of 75 GHz. We avoid the generation of SPM effects by keeping the power of the CUT sufficiently low, in this case, $P_{\mathrm{CUT}} = -20\,\mathrm{dBm}$, whereas the power of the pump was set to $P_{\mathrm{ch}} = 6\,\mathrm{dBm}$ to comfortably operate within the nonlinear regime and ensure that a sufficient amount of NLI was generated. We consider both pump and probe as root-raised cosine shaped coherent channels with roll-offs of 0.15 and channel symbol rates of 64 GBd. The CUT has been transmitted as a polarization-multiplexed (PM)-QPSK modulated signal, whereas the pump was launched with PM-QPSK and PM-16-QAM modulation formats to inspect modulation format dependence.

We considered two distinct line configurations; first propagating this spectral configuration through a 40-span periodic OLS operated in transparency, with ideal noiseless Erbium-doped fiber amplifiers (EDFA)s, henceforth denoted as the periodic scenario. Second, we propagated this spectral configuration over a single fiber span 40 separate times; we progressively applied predistortion to the pump equal to the dispersion accumulated by transmission through n preceding spans, representing all possible scenarios for an LP with an unknown history up to a maximum of $n = 40$ previously crossed fiber spans, denoting this collection of results the single-span simulations. We apply predistortion to both the pump and the probe, observing during this process that the probe predistortion has an entirely negligible effect upon the NLI generation of the pump. In the single-span scenario we additionally simulate a Gaussian modulated pump, representing the theoretical upper bound for NLI generation.

For both scenarios, these fibers had constant loss coefficients of $\alpha_{\mathrm{dB}} = 0.2\,\mathrm{dB/km}$, nonlinearity coefficients of $\gamma = 1.27$ 1/W/km, and the dispersions and lengths of each set of simulations were varied between $D = [4, 8, 16]\,\mathrm{ps\,/\,(nm{\cdot}km)}$ and $L_s = [50, 80, 100, 200]\,\mathrm{km}$, respectively. The NLI accumulation is retrieved by passing the signal at the end of each span through an ideal receiver, composed of an ideal dispersion compensation stage followed by a matched filter, and recovering only the average (constant) phase. The accumulated NLI power is then obtained by calculating $\mathrm{SNR}_{\mathrm{NL}}$ upon the received constellation. As a metric we normalize the NLI power with respect to $P_{\mathrm{CUT}}^2 P_{\mathrm{ch}}$, corresponding exactly to the NLI efficiency, η.

3. Results & Analysis

We present the combined results of the periodic and single-span simulations in Fig. 1a and Fig. 1a, for a QPSK and 16-QAM modulated pump in the $D = 16\,\mathrm{ps\,/\,(nm{\cdot}km)}$ line scenario, for all investigated span lengths. These results are given by the η gradient along the OLS, $\Delta\eta$, representing the amount of normalized NLI introduced by each span. We remark that this quantity is span length dependent for all scenarios under investigation. Furthermore, we obtain an identical result for all span lengths for the Gaussian modulated pump scenario, hence we present only the 200 km result. For both modulation formats we observe a difference between the NLI generation in the periodic simulation, previously seen in [4, 5]. Crucially, all single-span simulations tend towards an identical asymptote, corresponding to the level given by Gaussian modulated pump transmission. Practically, this behaviour represents the progressive *Gaussianization* of the pump as more predistortion is applied, with the Gaussian modulated scenario being a theoretically maximal limit [4, 5]. We additionally include the amount of NLI generated according to the GN model [10] for a single 200 km fiber span – this value always represents a conservative estimation of the single-span asymptote. We further highlight that a large transient is present within the first few spans for all configurations that corresponds to a large difference between the GN model/Gaussian modulation scenarios and

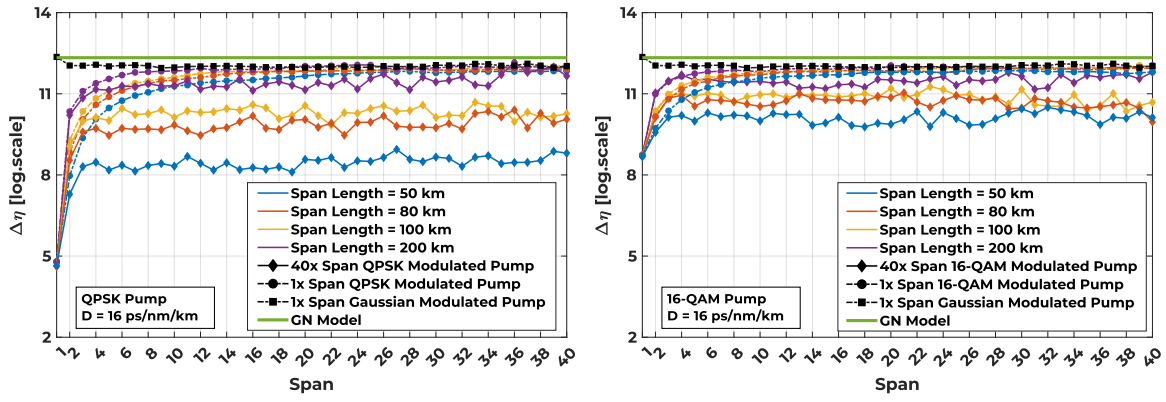

(a) (b)

Fig. 1: $\Delta\eta$ vs. the number of spans for an (a) QPSK and (b) 16-QAM modulated pump. The solid curves are the periodic line simulations. Dashed curves are the corresponding single-span results, with coloured circles for a QPSK/16-QAM modulated pump and black squares for a Gaussian modulated pump. The green lines are the levels given by the GN model.

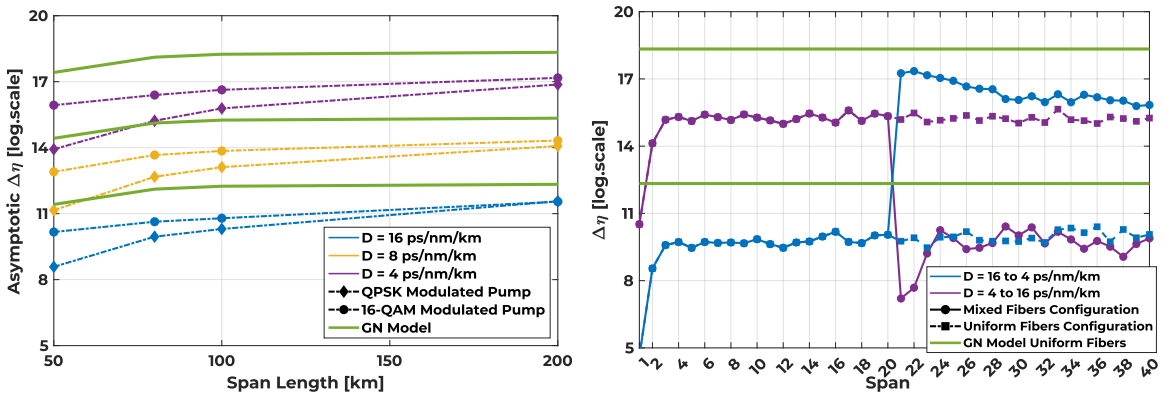

(a) (b)

Fig. 2: (a) the results of the periodic simulation campaign vs. span length, averaging the results of the last 20 spans, for QPSK and 16-QAM modulation formats. In (b) the results of the mixed fiber configurations along with levels that correspond to 40 uniform spans of each fiber dispersion. In both plots the green lines are the levels given by the GN model.

the periodic/single-span results.

Next, we present the asymptotic results for all line configurations within Fig. 2a, by taking the average $\Delta\eta$ over the last 20 spans of propagation and plotted against the span length. In these results it is visible that if the GN model is utilized as a conservative upper bound, there may be a large difference in $\Delta\eta$, for several cases being at least 2 dB, with this discrepancy decreasing proportionally to the fiber length. This corresponds to the maximum cross-channel NLI uncertainty induced by a channel with an unknown history and modulation format, demonstrating the fundamental statement that the GN model may be used as an always-conservative upper bound in this scenario. Otherwise, if the accumulated dispersion of the channel in question is known or able to be predicted, the use of a disaggregated model that takes this quantity into account as predistortion can be used to increase the accuracy of the NLI prediction. It is relevant to note that inaccuracies in the computations of the SNR_{NL} are mitigated due to its combined contribution with the OSNR to give the overall GSNR.

Additionally, we also show the NLI accumulation for two mixed fiber scenarios in Fig. 2b; here we consider an OLS consisting of 20 fiber spans with $D = 4\,\mathrm{ps/(nm{\cdot}km)}$ followed by 20 fiber spans with $D = 16\,\mathrm{ps/(nm{\cdot}km)}$, and vice versa. The change in fiber dispersion can clearly be seen, inducing a transient period where NLI is generated according to a clear rule: the transient is longer and lies above the asymptotic value for increasing chromatic dispersion values, and vice versa. The $\Delta\eta$ value tend towards at a stable value after the change in dispersion, highlighting that spatial disaggregation of the XPM is valid even for non-periodic OLSs. Furthermore, these transients are maximally quantified by the upper bound given by the GN model, allowing any additional NLI impairment to be accurately estimated.

4. Conclusion

We have shown the effect of fiber chromatic dispersion and modulation format upon cross-channel NLI generation using an extensive SSFM simulation campaign, demonstrating that the GN-model always provides a worst-case NLI prediction in the scenario where the history of the channel is unknown, such as for disaggregated network scenarios. We further investigated the behaviour of transients in a realistic terrestrial network scenario containing mixed-fiber OLSs.

Acknowledgment

This project has received funding from the European Union's Horizon 2020 research and innovation programme under the Marie Skłodowska-Curie grant agreement 814276.

References

1. Cisco Visual Networking Index: Forecast and Methodology, 2018, [Online]
2. V. Curri. Software-defined WDM optical transport in disaggregated open optical networks. *ICTON*, pp. 1-4, 2020.
3. A. Mecozzi, *et al*. Nonlinear Shannon limit in pseudolinear coherent systems. *JLT*, 30(12), pp.2011-2024, 2012.
4. R. Dar, *et al*. Properties of nonlinear noise in long, dispersion-uncompensated fiber links. *Optics Express*, 21(22), pp.25685-25699, 2013.
5. A. Carena, *et al*. EGN model of non-linear fiber propagation. *Optics express*, 22(13), pp.16335-16362, 2014.
6. L. Alahdab, *et al*. Alien wavelengths over optical transport networks. *JOCN*, 10(11), pp.878-888.
7. A. D'Amico, *et al*. Quality of transmission estimation for planning of disaggregated optical networks. *ONDM*, pp.1–3. IEEE, 2020.
8. E. London, *et al*. Simulative assessment of non-linear interference generation within disaggregated optical line systems. *OSA Continuum*, 3(12):3378–3389, 2020.
9. D. Pilori, *et al*. FFSS: The fast fiber simulator software. *ICTON*, , 2017.
10. P. Poggiolini, *et al*. The GN-model of fiber non-linear propagation and its applications *JLT*, 32(4), pp.694-721, 2013.